

UNCLASSIFIED

Defense Technical Information Center
Compilation Part Notice

ADP014101

TITLE: Computational Aero-Acoustic Studies of an Exhaust Diffuser

DISTRIBUTION: Approved for public release, distribution unlimited

Availability: Hard copy only.

This paper is part of the following report:

TITLE: Aging Mechanisms and Control. Symposium Part A -
Developments in Computational Aero- and Hydro-Acoustics. Symposium
Part B - Monitoring and Management of Gas Turbine Fleets for Extended
Life and Reduced Costs [Les mecanismes vieillissants et le controle]
[Symposium Partie A - Developpements dans le domaine de
l'aeroacoustique et l'hydroacoustique numeriques] [Symposium Partie B ...]

To order the complete compilation report, use: ADA415749

The component part is provided here to allow users access to individually authored sections
of proceedings, annals, symposia, etc. However, the component should be considered within
the context of the overall compilation report and not as a stand-alone technical report.

The following component part numbers comprise the compilation report:

ADP014092 thru ADP014141

UNCLASSIFIED

Computational Aero-Acoustic Studies of an Exhaust Diffuser

C. Jayatunga, G. Kroeff, J.F. Carrotte, J.J. McGuirk, B.A.T. Petersson

Department of Aeronautical and Automotive Engineering

Loughborough University

Loughborough LE11 3TU, UK

ABSTRACT.

The present paper describes work underway to develop a computational approach that can adequately simulate both the aerodynamic and acoustic behaviour of a typical exhaust diffuser/volute combination, such as are commonly used in industrial gas turbines for power generation use. An experimental rig was constructed to obtain a detailed understanding of the flow and acoustic properties of the system, and to provide guidance for computational modelling. Two different approaches are described for analysis of this system. The first uses CFD predictions carried out with a time-averaged RANS-based approach and a statistical turbulence model. Examples of the flow-field from this approach are presented. The second approach uses Large Eddy Simulation CFD, on a simplified geometry chosen on the basis of the experimental evidence, to provide information on the unsteady flow behaviour. This information is analysed and used to specify parameters for an acoustic analogy model. The acoustic model is also a simplified representation of the dominant noise source constructed from an experimentally derived viewpoint. The model is based on a ring of dipoles simulating the fluctuating pressure field associated with the unsteady vortex shedding/growth/merging process in the shear layer emerging from the diffuser exit. Spectral analysis of the unsteady velocity field provided by the LES calculation is used to determine amplitude, frequency dependence and phase relationships in the acoustic model. The basis of the model is described and sample outputs from both LES and acoustic model components are used to illustrate its performance.

INTRODUCTION.

Industrial gas turbines for electrical power generation are designed and supplied to the customer with an exhaust system that carries out a silencing function as well as providing for disposal of the exhaust gases into the surrounding atmosphere. The additional cost of the silencer can contribute significantly to the overall machine cost. This is particularly so if low frequency noise has to be removed. The design of the exhaust system must also comply with minimum ground footprint and packaging constraints, which usually require the exhaust flow to be turned from a horizontal flow path into the vertical to feed the silencer/exhaust stack. To reduce aerodynamic flow losses, which affect system efficiency, the annular duct downstream of the power turbine is connected to an annular diffuser/volute combination. An example of a typical geometry of such a system is shown in Figure 1. A short parallel-sectioned annular duct (formed between the machine outer casing and the central casing around the power transfer shaft) passes the flow to an annular diffuser. This is shown in Fig. 1 containing two rows of struts for structural purposes and with a scuffed exit to aid flow turning. The flow is then dumped into a volute, which directs the flow vertically into a rectangular cross-section duct feeding a downstream-located silencer. The flow characteristics associated with this geometry are strongly 3D and complex, containing recirculations, highly turbulent flow and possibly unsteady flow such as shedding from vanes and struts which are contained within the flow path. Currently, the interaction of these various flow features is poorly understood. The aerodynamic behaviour contributes to the overall system total pressure loss, but also acts as the origin of noise sources to create the range of frequencies that have subsequently to be silenced. Design optimisation methods, which can consider trade-offs between aerodynamic and acoustic aspects, are not currently available, leading to expensive testing at full-scale before an acceptable design is finalised.

Although the aerodynamic and acoustic behaviour of such components is extremely important in design optimisation of overall system performance, this seems to have received little attention to date. Compared with the extensive literature on the design of the diffuser systems elsewhere in the machine (e.g. in the main combustor [1] and [2]), exhaust diffusers have not been much studied. In terms of aerodynamic behaviour (loss reduction), evidence that the design is not straightforward was provided by the work of [3], where investigations of the need to install splitters in a short, wide-angle exhaust diffuser were reported. However, since this work was specifically aimed at performance of a particular existing engine design, little information of fundamental value emerged. On the acoustic front, some workers [4] have studied

noise generation due to vortex shedding from structural members (struts) in the flow path. It was shown that, since the struts were optimised for base-load operation, at lower operating power levels, where significant levels of swirl exit from the power turbine, large flow incidence angles on the struts lead to unsteady wakes and increased noise levels. Once again, however, no systematic understanding of the acoustic characteristics of general industrial gas-turbine exhaust diffusers evolved.

Fundamental acoustic studies of simple conical diffusers have been published ([5], [6], [7]). These authors have reported that separation in the diffuser is both a strong sound source in its own right, but also that the characteristics of the separation zone can be influenced by the acoustic properties of the duct system upstream and downstream of the diffuser. This implies for the present configuration, where the diffuser exit flow exhausts into a large volute box (see Fig. 1), that the jet shear layers created at diffuser discharge, the impingement of the jet on the volute back wall, and perhaps also the recirculation regions in the volute itself caused by flow turning, may all exert an influence on the acoustic behaviour.

In terms of aero-acoustic modelling, early work, trying to simulate the near-field processes that lead to jet noise, focussed on the vortex shedding process in the early-time period of jet shear layers. An example of this category of work is provided by [8]; a potential flow model for jet discharge was extended to allow for periodically shed ring vortices within the jet shear layer. The model was relatively successful in representing the mixing processes of the turbulent jet and also captured the correct spectral distribution of far-field noise. More recently, interest in terms of simulating jet noise (and other types of noise) has focused on development of Computational Aero-Acoustic (CAA) approaches. Two examples of some relevance to the present work may be found in [9] and [10]. The first has used the problem of turbulent boundary layer trailing edge noise to assess the current capabilities of CAA for this noise problem. The particular CAA approach adopted was based on a combination of: (i) Large Eddy Simulation (LES) CFD to capture the acoustic sources, and (ii) an acoustic analogy model based on the Lighthill formulation [11] to capture the propagation to the far-field. Predictions of far-field noise spectra were quite successful, but the authors pointed out the large computational cost of the LES calculation, even for this very simple geometry. In attempting to minimise the cost by choosing a solution domain as small as possible, the estimations of spanwise

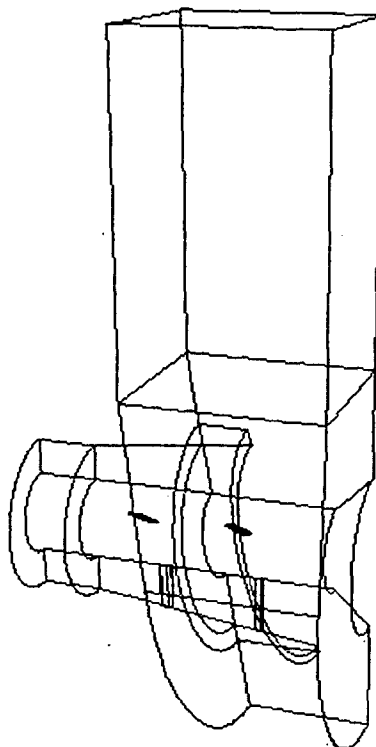


Figure 1 Typical diffuser and volute geometry

coherence of the noise deduced from the calculations showed that a wider computational domain should have been used, and this affected the accuracy of the predictions at the low frequency end. The CAA analysis reported in [10] was applied to a flow problem similar to one component of the present geometry. It considered a jet emerging from a circular duct into a larger space, although the discharged jet was still contained within a long circular duct of several times the jet diameter (this geometry has relevance to the human vocal tract if the initial jet diameter is considered to vary with time). Efforts were again made to minimise the computational costs, this time by considering only two-dimensional axi-symmetric flow. The emphasis of the work was placed on the demonstration of the ability of the high-order numerical techniques used to resolve the acoustic field. This was confirmed by the excellent agreement between the far-field acoustic pressure in the duct extracted directly from the CFD and results obtained from the same problem using the Fowcs-Williams and Hawkings version [12] of the acoustic analogy. Interestingly, the main noise source associated with a jet entering a larger space from a duct was found, by analysis of the directly computed acoustic signal, to be identified with a dipole source due to the unsteady forces exerted on the duct wall.

It is clear from the above that a complete understanding of the acoustic properties of flow inside the geometry shown in Fig. 1 will be difficult to achieve, and an adequate simulation model may have to take into account many factors. Accordingly, the methodology adopted in the present work was based around first conducting an experimental investigation of a scale model of the system under study to provide a clearer picture of its important aerodynamic and acoustic details. This approach mirrors that described in [13] for an aero-engine exhaust system. This work focussed on identification of the 'extra' noise sources that are known to exist in aero-engine exhausts in addition to the basic jet noise. It is noteworthy that, once again, similar to the findings of [10], dipole sources were found to dominate, this time associated with fluctuating pressures on the turbine outlet struts, with the source strength varying with the level of flow swirl. This study seemed to have several similarities with the present problem. An experimental facility was therefore designed and built and both flowfield and acoustic measurements undertaken, as described below. Based upon the findings of the experimental investigation, computational approaches for both steady (i.e. time-averaged) and unsteady flow and acoustic fields were selected and applied, and illustrative samples of these are also provided here.

EXPERIMENTAL INVESTIGATION.

Test Facility.

Figure 2 shows the essential details of the test facility constructed. This contains all important features of the exhaust diffuser problem described above. The rig was constructed from Perspex and represents the flow path from power turbine exit through to silencer inlet. Air is supplied to the rig via a centrifugal fan. To isolate the fan noise from the acoustic measurements being made, the fan was located within an acoustically lined enclosure isolated from the plenum chamber that fed the test rig

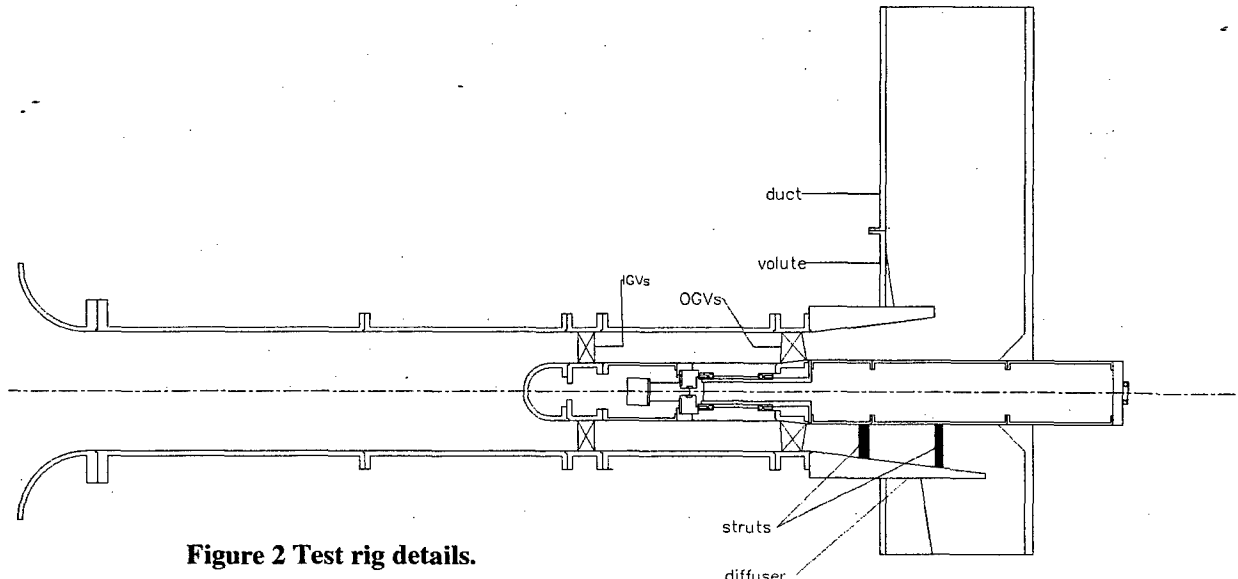


Figure 2 Test rig details.

via a bell-mouth, as shown in Fig. 2. Similar arrangements applied to the air exhausted from the rig into the test facility room. The rig incorporated all components downstream of the power turbine, i.e. a set of OGVs, a scarfed annular diffuser containing two rows of struts, and an exhaust volute. Inlet conditions to the exhaust system, simulating different power settings of the engine, were provided by 3 different sets of IGVs; these set the correct swirl level in the approach flow for 30%, 70% and 100% power conditions. The test rig was built in a modular fashion so that different components could be run in isolation or in (almost) any combination, i.e. with/without OGVs, with/without diffuser, with/without volute box, etc.

Aerodynamic Instrumentation and Measurements.

Measurements of the flowfield were made using five-hole pressure probes; measuring stations corresponded to OGV inlet, several planes within the diffuser and also within the volute. Radial traverses and also complete area traverses could be conducted (e.g. over a complete OGV blade passage to capture OGV wake behaviour). The instrumentation and motorised traverse gear were located within the centre shaft, part of which could rotate for accurate circumferential positioning. Space does not allow here a full survey of the data gathered, but Fig. 3 indicates a sample of the aerodynamic measurements taken. This shows three profiles of the time-mean axial velocity circumferentially averaged over the OGV blade pitch, for each level of inlet swirl. Flow conditions presented to the diffuser vary substantially with inlet swirl. At the 30% power condition, the incidence onto the OGV blades is high enough to cause separation near the blade tip. This is not the case for the 70% and 100% conditions, although at 70% there is still a region of low total pressure near the outer casing. As the flow passes down the diffuser, these inlet condition differences grow and the pitch-averaged profiles show a hub-biased shape at the low power conditions. It is likely that the diffuser is also separated over at least part of the circumference for the worst set of inflow conditions. In terms of the acoustic behaviour that will accompany these flow conditions, it is clear from the survey presented in the last section that diffuser separation will generate noise. The jet from the diffuser exit will also generate noise and the exit velocity profile in the jet is likely to be important; Fig. 3 shows that the profile shape at diffuser exit varies significantly, in particular the peak value of the axial velocity in the jet.

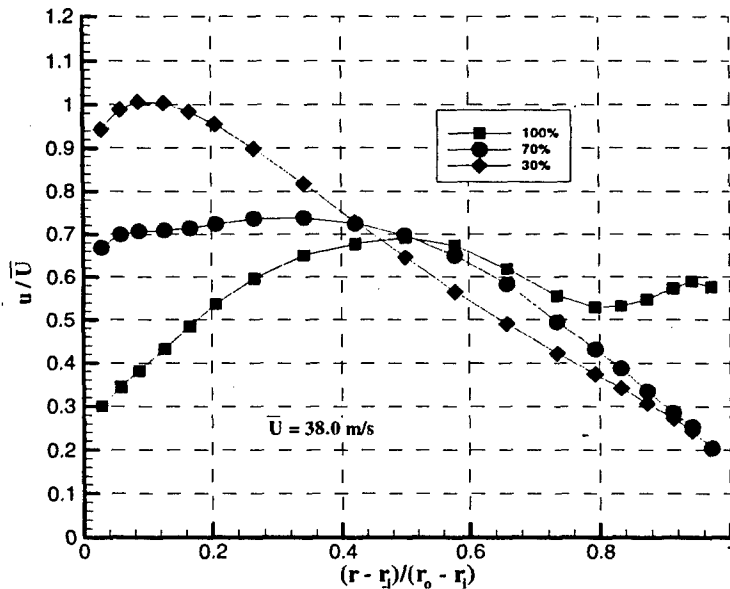


Figure 3 Circumferentially-averaged axial velocity profiles near diffuser exit.

Acoustic Instrumentation and Measurements.

Sound pressure measurements were taken with a 0.5 inch B&K microphone connected via pre-amplifiers to a Hewlett-Packard analyser; a foam windscreens was placed around the microphone to minimise interference from wind generated noise. The sound power for each configuration tested was obtained by averaging the sound pressure measurements taken at several fixed positions in the lab according to the relationship recommended in [14]. Before any measurements were taken, the acoustical properties of the lab containing the test facility were investigated by measuring its reverberation time and calculating the Schroeder frequency. These results showed that a quasi-diffuse sound field was present in the frequency range of interest and the Schroeder frequency was evaluated as 140 Hz. Since some frequencies of interest are below this level a large number of measurement points were used to obtain averages to guarantee the integrity of the results. Finally, background noise

measurements were taken to ensure that the background sound power levels were always at least 15dB below the measurements taken with the rig running.

The opportunity provided by the modular nature of the experimental facility was used to take acoustic measurements with various combinations of components present to identify whether the flow through/around particular components could be identified as a dominant aero-acoustic source, or whether that component could be viewed as acoustically unimportant. Fig. 4, for example, shows sound power level (SWL) measurements with and without the volute box present; all other components (IGVs, OGVs, struts, centre shaft, scuffed diffuser) were present and the data shown is for the 100% power level and an inlet Mach number of 0.08. There are several features of this spectrum which are characteristic of the system under study here. Firstly, the linear fall-off in SWL as frequency increases is expected if there is any jet-like contribution to the noise. The measurements

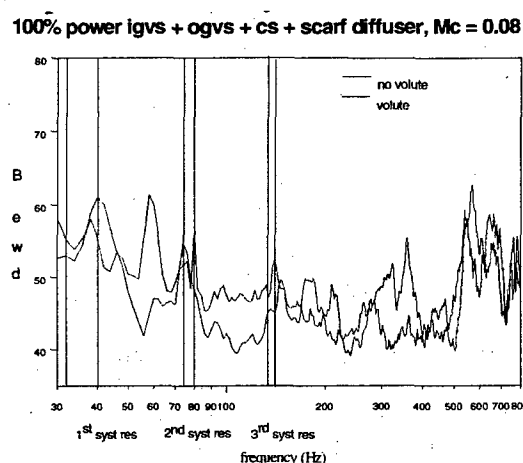


Figure 4 Sound power measurements with/without volute.

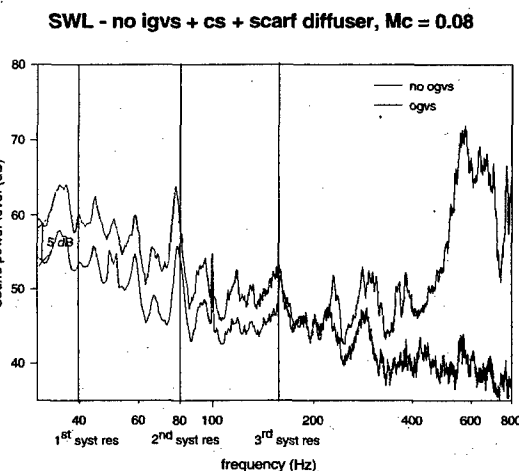


Figure 5 Sound power measurements with/without OGVs.

should also decrease at low frequency below a peak noise level expected from simple jet noise data to be at a Strouhal number of order 1. This would occur at a frequency of around 50Hz in the present measurements, however, the limited size and non-anechoic nature of the room in which the data were taken mean that this low frequency fall-off cannot be detected. Secondly, various duct modes are excited by the aerodynamic behaviour of the system. The first three plane wave harmonics are indicated in Fig. 4 (they differ slightly for with/without volute cases as the duct length changes), and peaks in the spectrum are clearly visible close to these frequencies. It is likely that the unsteady flow processes inside the diffuser, particularly if it separates, and in the near field of the jet shear layer at diffuser exit are the causes of the excitation. Finally, above around 200Hz, higher order modes of the duct system are cut on. Since the acoustic behaviour of the upstream duct system in the model experiment will be different from the engine geometry, these higher order modes are not of great interest, and most attention has been placed on the lower frequency portion of the SWL measurements. This is in any case the difficult portion to silence in the practical application. It can be seen that the presence of the volute in fact reduces the sound level. The likely explanation here is that the back pressure provided by the volute stabilises the flow in the diffuser as is often observed in main combustor pre-diffusers. These data therefore imply that the volute itself is not a fundamental noise source, in spite of the impingement processes and internal recirculations it contains. Figure 5 shows a similar story for the OGVs. In the absence of any OGVs the SWL data at low frequencies increase by around 5dB and the higher order modes are cut-off. This indicates, again consistent with observations made in combustor pre-diffusers, that the enhanced turbulence created in the OGV wakes has a beneficial effect on the diffuser flow. The higher order modes are identified as being connected with the blade-to-blade circumferential dimensions and are not present when the OGVs are removed. Once again however, the characteristic acoustic signature at the low frequency end is unchanged by the presence/absence of OGV blades and these may therefore also be discounted as a primary noise source; they are only influential in as far as they affect the diffuser flow.

Figure 6 confirms that the IGVs also exert very little dominant effect on the noise characteristics. With both IGVs and OGVs present there is a level increase of around 3dB in the frequency range of interest, presumably because of either interaction noise or diffuser flow influences. Once more, however, we can conclude that the IGV presence/absence is not fundamental to determining the low frequency noise characteristics.

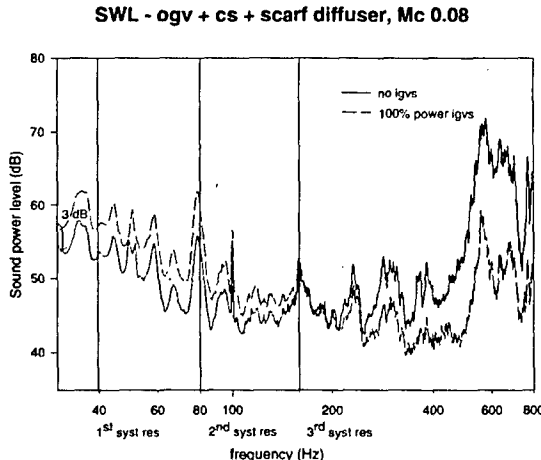


Figure 6 SWL data with/without IGVs.

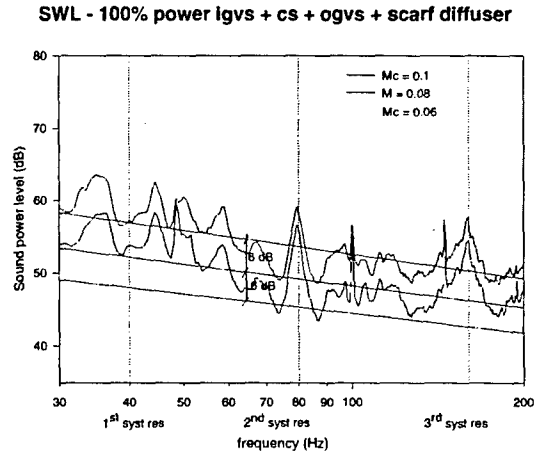


Figure 7 SWL data at varying Mach No.

The data in Figure 7 is the most illuminating of all. The configuration here contains all components except the volute box. The data were taken for varying flow rates, and three different inlet Mach numbers are indicated. Clearly at higher Mach numbers, as one would expect, the noise increases although again the overall characteristics remain unchanged. Of significance is the increment in dB level shown by the 'trend line' fitted to the data. A change in Mach number by +/- 0.02 leads to a change in noise level by +/- 6dB. This behaviour is exactly reproduced by a $(\text{vel})^6$ relationship. This provides strong evidence that the dominant noise source is dipole-like. This is exactly the same as the findings in [10] and [13], where, in both cases, a jet emerging from a duct into a larger space lead to a fluctuating pressure field on the solid surfaces of the jet-containing duct close to its exit, which then provided the dominant dipole source for noise radiation to the far-field. This finding has an important message for computational modelling. The acoustic measurements also imply that, perhaps in contrast to original expectations, neither separation from the blades or strut surfaces (singly or via interaction), nor separation/impingement processes in the volute, are of significance as dominant noise sources. This means that all these complications can be ignored in terms of acoustic modelling and emphasis should be placed on capturing the unsteady pressure field near the diffuser exit, which in all probability is strongly coupled to the unsteady vortex shedding in the emerging jet shear layer.

COMPUTATIONAL INVESTIGATION.

Time-averaged CFD – RANS Modelling.

If the full geometrical complexity of the system under consideration needs to be considered in any flowfield simulations, then it is clear that at present this can only practically be achieved by solving for the time-averaged flow using the Reynolds-Averaged-Navier-Stokes (RANS) formulation of the equations of motion and a statistical model of turbulence. The evidence from the experimental acoustics investigation implies that some simplifications are possible, but for aerodynamic assessment and accurate loss prediction, all system components are likely to need consideration. The approach adopted here is based on the methodology used previously in combustor aerodynamic simulations where complex geometry is also an important factor. Details of the code used and examples of its use are given in [15], only a brief description is provided here. The numerical methodology is based on a multi-block, cell-centred, finite-volume, and implicit solution of the RANS equations, using the standard high-Reynolds number $k-\epsilon$ model. For treatment of complex shaped domains, the Cartesian forms of the equations are transformed into a general 3D non-orthogonal curvilinear system and a structured grid was generated to fit the geometry using an elliptic pde method.

Two examples of the predictions obtained for the diffuser/volute combination are given in Figs. 8 and 9. The inlet conditions for this calculation were taken from the experimental measurements, since it is known, as commented above, that accurate aerodynamic predictions of diffuser performance require the OGV wakes and associated turbulence generation to be taken into account. Fig. 8 shows the mixing out of the vane wakes as they pass down the diffuser; their behaviour influences the level of pressure recovery achieved by the diffuser and the accompanying level of loss. As can be seen in Fig. 8, the interaction between the vane wakes and the adverse pressure gradient in the diffuser determine

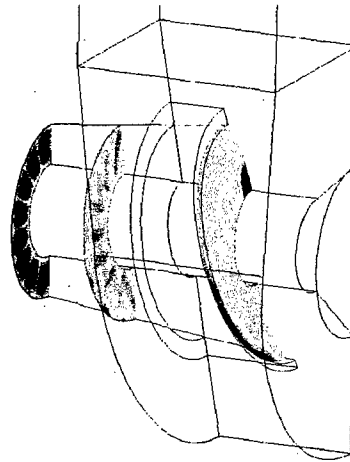


Figure 8 OGV wake mixing inside diffuser.

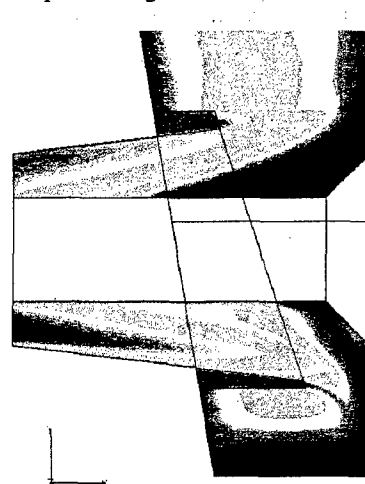


Figure 9 Axial velocity contours at diffuser exit.

any regions of separation present, and this calculation implies that there is separation inside the current diffuser, initially on the outer wall, but eventually at diffuser exit on the upper part of the central shaft. Fig. 9 shows a close-up view of this. If this steady state calculation is an accurate representation of events at diffuser exit then it is clear that the unsteady nature of the separation and the emerging jet will dominate the unsteady pressure field on the diffuser walls, which is believed to be the primary dipole-like noise source.

Unsteady CFD – LES Modelling.

It is clear that no information about the unsteady flow and pressure field can be deduced from the above CFD approach. For this, following the work of [9], the Large Eddy Simulation (LES) methodology has been selected for use. Since the acoustic measurements have shown that many features of the geometry do not significantly influence the primary noise characteristics, a simplified geometry has been chosen for the LES study. Initially only the annular diffuser and the annular jet, which emerges at diffuser exit into a larger space, have been considered. An unscarfed, plane-ended diffuser has been calculated in the first instance since it was much easier to generate a high quality orthogonal mesh for this geometry. The LES methodology is fully described in [16] and only indicative results of the predictions are presented here. In the first instance, only a simple eddy viscosity based Smagorinsky sub-grid-scale model has been used for the non-resolved eddies. Fig. 10 shows an instantaneous snapshot of the axial velocity contours. It is very clear to see that the LES calculation has now captured the fluctuating eddy structure associated with the jet shear layers in a way that no RANS prediction can. The jet spreads as it penetrates into the enclosure outside of the diffuser and the air in this enclosure is recirculated

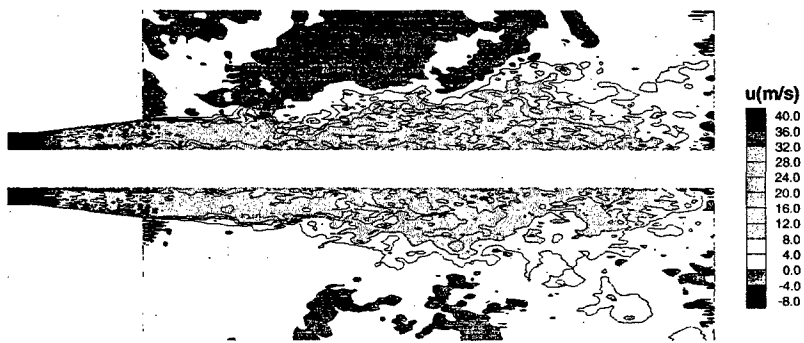


Figure 10 LES prediction of instantaneous velocity.

and entrained into the jet. Clearly a single snapshot cannot capture the unsteady flow features adequately. Fig.11 is therefore provided to indicate the time history of velocity at just one selected point, chosen to be at the exit plane and near the outer diffuser wall in the upper half of Fig. 10. The range of frequencies present in the time history is very clear, caused by the range of eddy sizes resolved by the grid used in the LES calculation. This range of fluctuating motions may also be visualised by performing a spectral analysis of time histories, as shown in Fig. 12 for both velocity and pressure at the selected point. The velocity spectrum indicates a range of frequencies from around 10 to 1 kHz, with most energy in the O(100Hz) range.

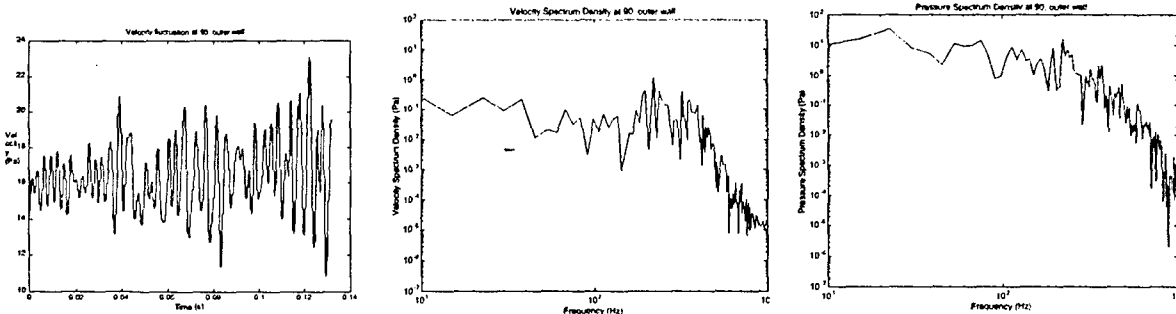


Figure 11 Time history of velocity from LES predictions.

Figure 12 Spectral analysis of pressure and velocity time histories.

There is some evidence of a separate peak at 200Hz although the sample length is not quite long enough to confirm this absolutely. The pressure spectrum shows that the unsteady pressure on the duct wall is captured by the LES approach. This time-dependant information is of course precisely the information that can form the route to linking the aerodynamic and acoustic problems. Although the above analysis has not been carried out for exactly the geometric system under study, it is believed the calculations are representative and are sufficient to illustrate how this information may be used to feed into an acoustic model of the system.

Sound Field – Acoustic Modelling.

The unsteady results of the LES calculation could be used to drive a Lighthill-equation acoustic analogy model to simulate the sound propagation to the far field, as shown by [10]. However, the dominance of the dipole characteristic indicated in the acoustic measurements, and the identification of this with the unsteady pressure field on the diffuser duct wall, has encouraged a simpler approach to acoustic modelling to be attempted initially. A single dipole ring located at diffuser exit is postulated to represent the primary acoustic sources adequately. The parameters of the ring (number and distribution of dipoles, strength and phase relationships between individual dipoles in the ring) may all be varied, but the present investigation has concentrated on demonstrating the typical output of a simple dipole ring model, driven via information deduced from the LES predictions. The dipole ring is modelled as a sum of N discrete radially directed dipoles on a circle of radius r_0 centred on the geometric centre of the annular diffuser exit, and equally spaced from each other around the ring. For the present calculation r_0 has been taken as the diffuser outer radius. The acoustic pressure at some point in the far field for the n th individual dipole is given by:

$$p_n(\underline{r}, k, t) = \operatorname{Re}(\hat{p}_n(\underline{r}, k) e^{-i\omega t})$$

Where \underline{r} represents the vector between the dipole and the far field point and k is wave number ($k=\omega/c$). The complex amplitude of the acoustic pressure is:

$$\hat{p}_n(\underline{r}, k) = -k^2 \hat{D}_n(k) \frac{\rho c}{4\pi |\underline{r}|} \cos \phi_n \left(1 + \frac{i}{k |\underline{r}|} \right) e^{ik|\underline{r}|}$$

ρ and c are fluid density and sound speed respectively, \hat{D}_n is the complex dipole source strength (volume velocity), which has a frequency dependent amplitude and phase, both of which are to be specified via LES information, the angle ϕ_n is the angle between the n th dipole and the vector to the

far field point. The acoustic pressure and velocity at any far field point due to the presence of all N dipoles in the ring are given by:

$$\hat{p}_f(\underline{r}, k) = \sum_{n=1}^N \hat{p}_n \quad \hat{\mathbf{v}}_f(\underline{r}, k) = \frac{1}{i\rho k c} \operatorname{grad}(\hat{p}_f)$$

and the sound intensity at any far field point may be calculated from:

$$I(\underline{r}, k) = \frac{1}{2} (\hat{p}_f \cdot \hat{\mathbf{v}}_f^* + \hat{p}_f^* \cdot \hat{\mathbf{v}}_f)$$

Where an asterisk indicates a complex conjugate. In the example shown below, 8 dipoles have been considered and at each one the frequency dependent amplitude and phase information have been obtained by analysing the LES predictions at the corresponding point at diffuser exit. The Fourier transform of the velocity time history at each point yields the information needed to specify \hat{D}_n , the source strength is calculated using this velocity information and allocating a fraction of the dipole ring area to each dipole.

Fig. 13 shows a sound intensity plot for around a circle of radius 2m and centred on the axis of the dipole ring (approximately the location of the SWL measurements reported earlier). The plot is for a frequency of 83Hz, but the strong dipole-like character is present over a range of frequencies. At present the reason for the orientation of the dipole is unclear. Finally, the far field acoustic pressures produced by the dipole ring may be analysed to produce a sound pressure level plot; this is shown in Fig. 14 for a point on the 2m radius and above the top of the diffuser. This spectrum shows a peak at between 200 and 300 Hz which is where the velocity spectrum from the LES indicated a possible peak, but further analysis of the acoustic model predictions are required to confirm this.

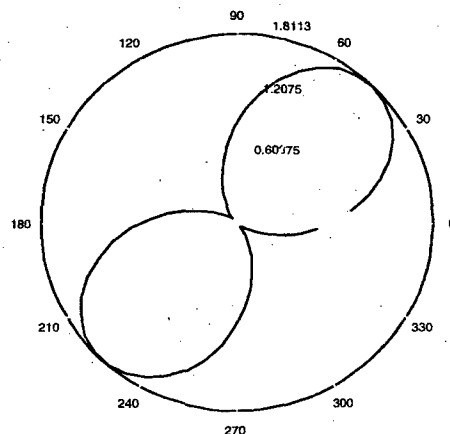


Figure 13 Sound Intensity plot deduced from acoustic model.

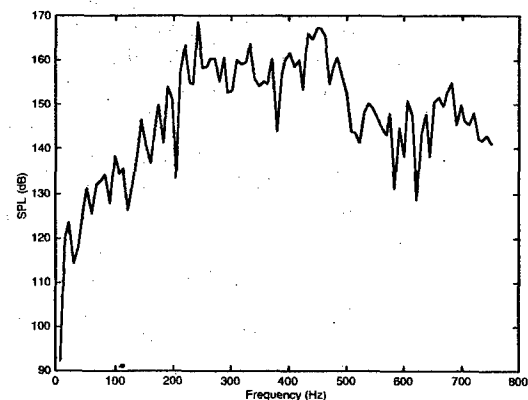


Figure 14 SPL level deduced from acoustic model.

SUMMARY/CONCLUSIONS.

This paper has summarised work carried out to construct a computational aero-acoustic model of a diffuser and volute combination relevant to industrial exhaust systems. The complex nature of the aerodynamic behaviour of this system and the many possible acoustic sources encouraged an initial experimental investigation to characterise the flowfield and eliminate some of the possible noise sources. This lead to a belief that any acoustic model should concentrate on the unsteady aerodynamic processes of possible diffuser separation and on vortex shedding/jet shear layer phenomena at diffuser exit. A RANS-based CFD calculation of the complete geometry showed that separation was predicted in the vicinity of the centre shaft, but this modelling approach allowed no information to be obtained on the unsteady flowfield. An LES calculation in a simplified geometry was then carried out. This methodology shows significant promise for providing the unsteady information so important for predicting the acoustic behaviour. To indicate how the LES-deduced unsteady flow information might

be used, a simplified acoustic model was constructed based on the assumption of a ring of dipoles simulating the important aerodynamic processes at diffuser exit. Frequency dependent amplitude and phase information for each dipole in the ring were deduced from the LES results. Illustrative examples of sound intensity and sound power level spectra were provided to indicate how this model could be used to provide such information. This approach is viewed as worthy of future study based on the present results.

ACKNOWLEDGEMENTS.

The work reported here has been conducted within the Rolls-Royce University Technology Centre in Combustion Aerodynamics at Loughborough University. The authors gratefully acknowledge support and many useful technical discussions with colleagues at Loughborough, Rolls-Royce (Ansty), and Rolls-Royce (Derby).

REFERENCES.

- [1] D Zhou, T Wang, W R Ryan, "Cold flow computations for the diffuser-combustor section of an industrial gas-turbine", ASME paper 96-GT-513, 41st Int. Gas Turbine and Aeroengine Congress, Birmingham, UK, 1996.
- [2] A K Agrawal, J S Kaput, T Yang, "Flow interactions in the combustor-diffuser system of industrial gas-turbines", ASME paper 96-GT-454, 41st Int. Gas Turbine and Aeroengine Congress, Birmingham, UK, 1996.
- [3] H Harris, I Pineiro, T Norris, "A performance evaluation of a three splitter diffuser and a vaneless diffuser installed on the power turbine exhaust of a TF40B gas turbine", 43rd Int. Gas turbine and Aeroengine Congress, Stockholm, Sweden, 1998.
- [4] T F Fric, R Villareal, R O Auer, M L James, D Ozgur, T K Stanley, "Vortes shedding from struts in an annular exhaust diffuser", ASME paper 96-GT-XXX 41st Int. Gas Turbine and Aeroengine Congress, Birmingham, UK, 1996.
- [5] A H M Kwang, A P Dowling, "Unsteady flow in diffusers", ASME Jnl. of Fluids Eng. Vol. 116, pp 842-847, 1994.
- [6] K R Fehse, W Neise, "Low frequency sound generated by flow separation in a diffuser", Eur. Jnl. Of Mechs-B-Fluids, Vol. 19, pp 637-652, 2000.
- [7] L van Lier, S Dequard, A Hirschberg, J Gorter, "Aero-acoustics of diffusers: an experimental study of typical industrial diffusers at Reynolds numbers $0(10^5)$ ", Jnl. of Acoustical Soc. Of America , Vol. 109, pp 108-115, 2001.
- [8] P O A L Davies, J C Hardin, A V J Edwards, J P Mason, "A potential flow model for calculation of jet noise", Prog. In Astronautics and Aeronautics, Vol. 43, pp 91-106, 1975.
- [9] M Wang, P Moin, "Computation of trailing-edge flow and noise using Large Eddy Simulation", AIAA Jnl., Vol. 38, pp 2201-2209, 2000.
- [10] W Zhou, S M Frankel, L Mongeau, "Computational aero-acoustics of an axi-symmetric jet in a variable area duct", AIAA paper 01-2788, 31st AIAA Dynamics Conference, Anaheim, USA, June, 2001.
- [11] M J Lighthill, "On sound generated aerodynamically", Proc. Roy. Soc., Vol. 211, pp564-587, 1952.
- [12] J E Fowcs-Williams and D L Hawkings, "Sound generation by turbulence and surfaces in arbitrary motion", Proc. Roy. Soc., Vol. 264, pp321-342, 1969.
- [13] W D Bryce and R C K Stevens, "An investigation of the noise from a scale model of an engine exhaust system", AIAA Paper 75-459, AIAA 2nd Aero-Acoustics Conference, Hampton, VA, USA, 1975.
- [14] J R Hassall and K Zaveri, "Acoustic Noise Measurements", Brue and Kjaer Publication, 1988.
- [15] J J McGuirk and A Spencer, "Coupled and uncoupled CFD prediction of the characteristics of jets from combustor air admission ports", ASME Jnl. Of Engineering for Gas Turbines and Power, Vol. 123, pp 327 – 332, 2001.
- [16] G Tang, Z Yang, J J McGuirk, "LES predictions of aerodynamic phenomena in LPP combustors", ASME paper 2001-GT-465, 46th Int. Gas Turbine and Aeroengine Congress, New Orleans, LA, USA, June 2001